The adaptor molecule CARD9 is essential for tuberculosis control

Anca Dorhoi,[1] Christiane Desel,[1] Vladimir Yeremeev,[1] Lydia Pradl,[1] Volker Brinkmann,[1] Hans-Joachim Mollenkopf,[1] Karin Hanke,[1] Olaf Gross,[2] Jürgen Ruland,[2] and Stefan H.E. Kaufmann[1]

[1]Max Planck Institute for Infection Biology, Department of Immunology, 10117 Berlin, Germany
[2]III. Medizinische Klinik, Klinikum rechts der Isar, Technische Universität München, 81675 München, Germany

The cross talk between host and pathogen starts with recognition of bacterial signatures through pattern recognition receptors (PRRs), which mobilize downstream signaling cascades. We investigated the role of the cytosolic adaptor caspase recruitment domain family, member 9 (CARD9) in tuberculosis. This adaptor was critical for full activation of innate immunity by converging signals downstream of multiple PRRs. *Card9*$^{-/-}$ mice succumbed early after aerosol infection, with higher mycobacterial burden, pyogranulomatous pneumonia, accelerated granulocyte recruitment, and higher abundance of proinflammatory cytokines and granulocyte colony-stimulating factor (G-CSF) in serum and lung. Neutralization of G-CSF and neutrophil depletion significantly prolonged survival, indicating that an exacerbated systemic inflammatory disease triggered lethality of *Card9*$^{-/-}$ mice. CARD9 deficiency had no apparent effect on T cell responses, but a marked impact on the hematopoietic compartment. *Card9*$^{-/-}$ granulocytes failed to produce IL-10 after *Mycobaterium tuberculosis* infection, suggesting that an absent antiinflammatory feedback loop accounted for granulocyte-dominated pathology, uncontrolled bacterial replication, and, ultimately, death of infected *Card9*$^{-/-}$ mice. Our data provide evidence that deregulated innate responses trigger excessive lung inflammation and demonstrate a pivotal role of CARD9 signaling in autonomous innate host defense against tuberculosis.

CORRESPONDENCE
Stefan H.E. Kaufmann:
kaufmann@mpiib-berlin.mpg.de

Abbreviations used: AEC, alveolar epithelial cell; AG, arabinogalactan; BMDC, BM-derived DC; BMDM, BM-derived macrophage; CARD9, caspase recruitment domain family, member 9; CLR, C-type lectin receptor; DTH, delayed-type hypersensitivity; G-CSF, granulocyte colony-stimulating factor; INH, isoniazid; KC, keritinocyte-derived chenokine; mAGP, mycolyl-AG PG; MAME, mycolic acid methyl ester; MPO, myeloperoxidase; MTB, *Mycobacterium tuberculosis*; NLRs, NOD-like receptors; PG, peptidoglycan; p.i., post infection; PMN, polymorphonuclear neutrophil; PRR, pattern recognition receptor; RIF, rifampicin; TB, tuberculosis; TDM, trehalose dimycolate; TLR, Toll-like receptor.

Tuberculosis (TB) is a communicable disease that afflicts 9 million people and claims 2 million lives annually (WHO, 2008). The disease is caused by the intracellular pathogen *Mycobacterium tuberculosis* (MTB) which persists in resting macrophages. Protective immunity against TB depends on robust responses of type 1 helper T (Th1) cells that achieve bacterial containment, but not sterile eradication (Flynn and Chan, 2001).

Once inhaled, MTB is recognized by pattern recognition receptors (PRRs), which are nonclonally expressed by macrophages, DCs, or epithelial cells. After receptor engagement, PRRs transduce signals to adaptor molecules, which mobilize appropriate defense mechanisms. To date, several key adaptor molecules have been characterized (Ishii et al., 2008): MyD88 collects signals from most Toll-like receptors (TLRs), TRIF primarily from TLR-3/4, RIP2 from nucleotide-binding oligomerization domain (NOD)–like receptors (NLRs, like NOD1 and 2), and the recently described caspase recruitment domain family, member 9 (CARD9) from some TLRs, as well as from NOD2 and dectin-1 (Gross et al., 2006; Hara et al., 2007; Hsu et al., 2007). These adaptors can activate NF-κB, MAPKK, or IRFs, and the master regulators for synthesis of cytokine and type I IFNs. MTB is a complex prokaryote consisting of myriads of structurally different molecules that can be recognized by different PRRs. Effects of single or multiple deletions of TLRs (TLR 2, 4 and 9; Reiling et al., 2002; Hölscher et al., 2008; Reiling et al., 2008) or NLRs (NOD2; Gandotra et al., 2007) on murine TB are minimal. Moreover, although

V. Yeremeev's present address is Dept. of Immunology, Central Institute for Tuberculosis, 107564 Moscow, Russia.

O. Gross's present address is Dept. of Biochemistry, University of Lausanne, 1066 Epalinges, Switzerland.

The Rockefeller University Press $30.00
J. Exp. Med. Vol. 207 No. 4 777-792
www.jem.org/cgi/doi/10.1084/jem.20090067

TLR-2 and NOD2 are nonredundant receptors for MTB recognition in vitro (Ferwerda et al., 2005), double KO mice for these receptors control lung infection efficiently (Gandotra et al., 2007). Yet, animals deficient in the MyD88–IL-1R pathway fail to control TB (Fremond et al., 2004, 2007). Consistent with these observations and considering the structural diversity of the mycobacterial cell wall, "adaptor check points" rather than "receptor check points" are essential for control of MTB in innate immune cells.

PRRs involved in MTB recognition not only use MyD88-dependent, but also MyD88-independent pathways (Shi et al., 2003; Fortune et al., 2004; Schnappinger et al., 2006), and therefore additional adaptors await identification. The involvement of the adaptor CARD9 was recently reported in early recognition and defense against *Candida sp.* (Gross et al., 2006) and *Listeria monocytogenes* (Hsu et al., 2007). It samples signals from diverse classes of receptors, such as C-type lectin receptors (CLRs) and other ITAM-based receptors, RIG-I–like helicases (Poeck et al., 2010), NLRs, and TLRs (Hara et al., 2007), and can act independently of MyD88. Here, we investigated whether CARD9 is involved in control of TB.

In the mouse model of pulmonary TB we demonstrate a crucial role of CARD9 in control of MTB. We provide compelling evidence for a critical role of CARD9 as a central adaptor downstream of multiple receptors involved in MTB recognition. Absence of CARD9 resulted in a lethal systemic inflammatory disease dominated by augmented cell death in the lung and marked neutrophil pathology. In contrast, T cell responses were apparently not affected by this deficiency. Survival of *Card9*$^{-/-}$ mice was prolonged by granulocyte colony-stimulating factor (G-CSF) neutralization or granulocyte depletion. Similar effects were achieved after MTB curtailment by antibiotic treatment before or after the neutrophilic response had been initiated. Failure to control inflammation in KO mice was linked to abolished secretion of IL-10 in MTB-infected *Card9*$^{-/-}$ granulocytes and inability to dampen inflammation. We propose a central role for CARD9 in control of TB and assume that *Card9* deficiency causes aberrant systemic inflammation culminating in lethal lung damage.

RESULTS

Fatal tuberculosis in *Card9*$^{-/-}$ mice

Aerosol infection with virulent strain MTB H37Rv caused rapid death of *Card9*$^{-/-}$ mice (Fig. 1 A). Diseased animals gradually lost weight (Fig. S1) and started to succumb at 26 d post infection (p.i.). Over a wide range of the bacterial inoculum (100–450 CFUs) we observed a remarkable susceptibility of *Card9*$^{-/-}$ mice, which did not survive beyond 34 d p.i. in any of the experimental settings.

Lung bacterial burdens were significantly higher in *Card9*$^{-/-}$ mice (Fig. 1 B), and Ziehl-Neelsen staining of infected lungs confirmed CFU results (Fig. 1 C). Histological examination revealed profound tissue damage in susceptible animals (Fig. 1, D–F), characterized by acute pneumonia with accelerated accumulation of inflammatory cells. Parenchyma appeared disorganized with multiple necrotic foci and lacked typical granulomatous appearance. Large infiltrates were often surrounded by emphysematous tissue and rarely by functional alveoli. Spleen pathology did not significantly differ between mouse strains (Fig. S2). Because the lung architecture was massively altered, we assessed impact of *Card9* deficiency on cell death. iNOS expression was determined as a major antimicrobial effector molecule in mice. In accordance with the results obtained for NO serum levels (Fig. S2), iNOS immunostaining revealed no apparent differences between WT and KO animals. The more intense TUNEL signals in the *Card9*$^{-/-}$ mice indicated differential apoptotic cell death. We also detected a different TUNEL staining pattern. In WT tissues, apoptotic signals were nuclear, whereas extracellular, interstitial TUNEL-positive material preponderated in *Card9*$^{-/-}$ lungs, indicative of secondary necrosis. Thus, increased cell death events in inflamed lungs of *Card9*$^{-/-}$ mice correlated with TB susceptibility.

Defective responses to MTB infection in *Card9*$^{-/-}$ antigen-presenting cells

To define the mechanisms responsible for the high susceptibility to TB in *Card9*$^{-/-}$ mice, we generated BM-derived macrophages (BMDMs) and BM-derived DCs (BMDCs) and infected them with MTB H37Rv. *Card9*$^{-/-}$ BMDMs produced similar NO levels as WT cells (Fig. 2 C), and were neither impaired in internalization (Fig. 2 B) nor in killing of MTB after IFN-γ activation (Fig. 2 A). Strong evidence for increased cell death in lungs of *Card9*$^{-/-}$ mice prompted us to determine whether deficient BMDMs showed accelerated cell death after MTB encounter. Nucleosome enrichment in postnuclear fractions did not differ, suggesting similar frequencies of apoptotic cell death in WT and KO cells after MTB infection (Fig. 2 D). Clearance of apoptotic cells by *Card9*$^{-/-}$ BMDMs was also not impaired (Fig. S3).

To monitor cell activation status we measured cytokine levels in culture supernatants. *Card9*$^{-/-}$ BMDMs were impaired in synthesis of the proinflammatory cytokines TNF, IL-6, and CCL5 and produced less IL-12 compared with WT cells (Fig. 2 E). Moreover, they were defective in IL-1β release (Fig. 2 F). A similar response pattern of infected BMDCs (depicted for IL-1β and TNF) and lower IL-12p40 abundance was recorded (Fig. S4). We hesitate to draw conclusions on the biological meaning of IL-12 levels in DC supernatants because of the high background caused by MACS separation of the cells. However, we do assume that CARD9 is critical for adequate activation of innate immune cells after MTB recognition.

CARD9 as central adaptor in MTB recognition

CARD9 is involved in multiple signaling pathways, downstream of different classes of PRRs (Ishii et al., 2008). To characterize receptors upstream of CARD9 involved in APC responses to MTB, we performed experiments using heat-killed MTB or blocking phagocytosis. The differential activation after cytochalasin treatment or after recognition of

heat-killed MTB confirmed our experiments with live MTB (Fig. 3 A). We conclude that the CARD9 pathway is important for sensing MTB lipoglycan compounds through cell surface PRRs.

Because the relevance of TLRs in TB is well established (Reiling et al., 2008), we focused on dectin-1/Syk–dependent macrophage activation by MTB. We treated cells with either 500 μg/ml laminarin or 1–10 μM piceatannol 1 h before

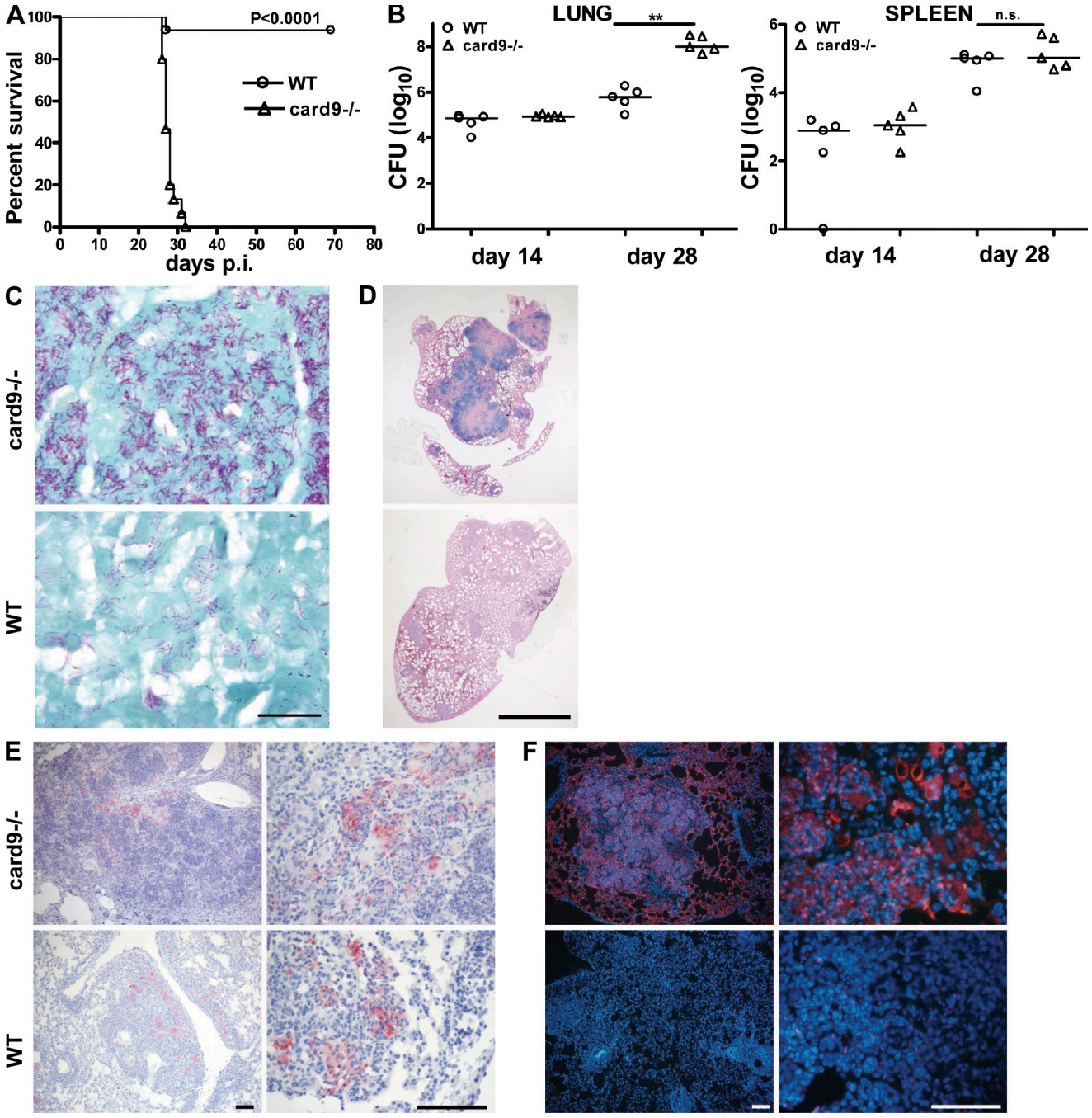

Figure 1. *Card9*$^{-/-}$ mice fail to control pulmonary tuberculosis. (A) Survival of WT and *Card9*$^{-/-}$ mice (n = 15) after aerosol infection with virulent MTB H37Rv (450 CFUs), Kaplan-Meier curves, and log-rank test. (B) Bacterial burdens in lungs and spleens of infected animals (n = 5). Data from one of four experiments, Mann-Whitney test for statistic analysis. (C) Ziehl-Neelsen staining of acid fast bacilli in lungs of infected mice. (D–F) Histopathology of lungs; Giemsa staining (D) of paraffin-embedded tissue showed acute pneumonia with multiple necrotic foci in susceptible mice; immunostaining for iNOS did not reveal major differences (E); TUNEL staining revealed accelerated cell death in Card9$^{-/-}$ mice (F). TUNEL-TMred and nuclei are DAPI stained. Tissue were collected at 28 d p.i. Data in C–F are representative of two independent experiments (n = 5). Bars: (C) 20 μm; (D) 2.5 mm; (E) 200 μm; (F) 100 μm. **, $P < 0.01$.

infection. Both laminarin (β-glucan, thus blocking dectin-1) and piceatanol (syk inhibitor) specifically blocked TNF and IL-6 synthesis, leaving MTB internalization unaffected (Fig. S5 A). Thus, dectin-1 signaling was involved in proinflammatory responses against MTB (Fig. 3 B). Next, we stimulated BMDMs and DCs with the following MTB-derived molecules: peptidoglycan (PG), mycolyl-arabinogalactan (AG) PG (mAGP), manLam, and trehalose dimycolate (TDM). We measured levels of TNF, IL-10 (Fig. 3 C), IL-12, and IL-6 24 h after stimulation. Scant cell activation was

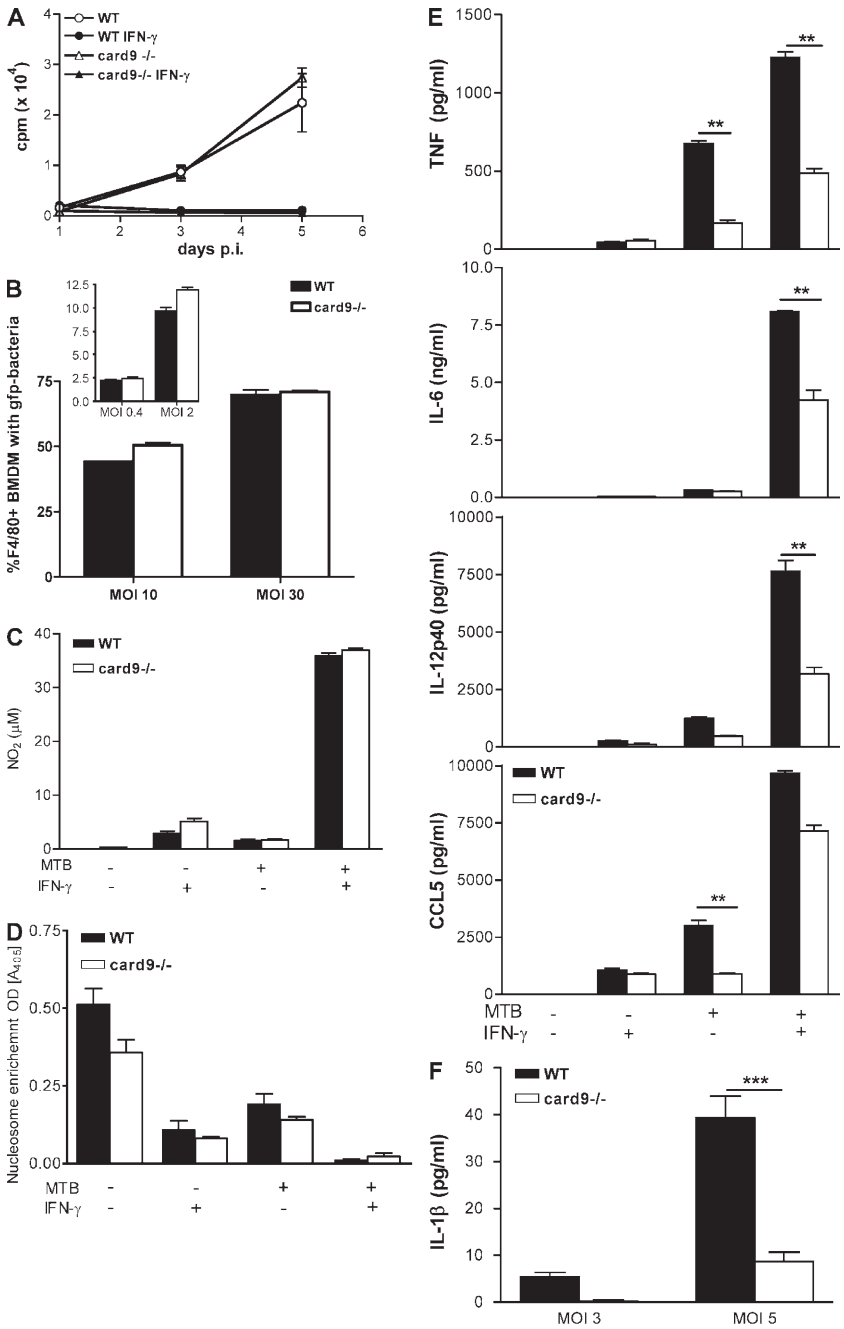

Figure 2. *Card9*$^{-/-}$ BMDMs control MTB despite impaired cytokine synthesis. (A) BMDMs from WT and *Card9*$^{-/-}$ mice were infected with MTB H37Rv at MOI 5 and bacterial multiplication was assed by [^{3}H]Uracil incorporation. (B) WT and *Card9*$^{-/-}$ BMDMs were infected with gfp-BCG at different MOI and mycobacterial uptake was monitored by FACS analysis of the F4/80$^+$ population, insert lower MOI (0.4 and 2) were assessed as well. (C) *Card9*$^{-/-}$ BMDMs were not hampered in NO release, NO in cell culture supernatants was assessed by Griess reaction. (D) Cell death after MTB infection was evaluated by nucleosome enrichment in the post-nuclear fraction using ELISA. (E) Cytokines in supernatants of infected cell were determined by ELISA. Data are mean ± SEM of two experiments with six replicates each (A) or are representative of three independent experiments with three replicates each (B–E). **, $P < 0.01$; ***, $P < 0.001$, Student's *t* test.

observed for manLam and TDM (unpublished data). This observation is in agreement with studies that investigated TDM/TDB activity on myeloid cells and reported minimal cytokine release at 24 h, but substantial production at later timepoints (Werninghaus et al., 2009). Clear differences were measured for mAGP (Fig. 3 C and Fig. S5, B and C). The mAGP-triggered cytokine synthesis in macrophages depends on NOD2, an intracellular sensor for PG (Fortune et al., 2004; Gandotra et al., 2007). Mycolic acid methyl esters (MAMEs) and AG, which are constituents of mAGP, induced scant TNF release (unpublished data). Overall, our data suggest that the CARD9 adaptor collects signals from various PRRs, including dectin-1, and NOD2 during MTB infection, reemphasizing its critical role in control of innate immunity.

Systemic inflammatory disease in absence of CARD9 despite apparently normal T cell responses

To further characterize the role of CARD9 in TB in vivo, we performed a detailed analysis of innate and adaptive cell responses in the lungs and spleens of infected mice. Aerosol infection with a low inoculum (70 CFUs) did not reveal apparent differences in T cell subpopulations recruited to the lung at day 14 p.i. Disease progression did not alter the ratio of $CD4^+/CD8^+$ cells in *Card9*$^{-/-}$ versus WT mice (Fig. 4 A). Moreover, the frequencies of PepA tetramer-positive $CD8^+$ T cells (Fig. 4 B) and $FoxP3^+$ T lymphocytes (unpublished data) did not differ in *Card9*$^{-/-}$ and WT mice. Next, we determined T cell functions. Cytokine production (IL-2, IFN-γ, TNF, and IL-17) was not altered consistently (Fig. 4 B and Fig. S6). Moreover, in preliminary experiments CARD9 KO

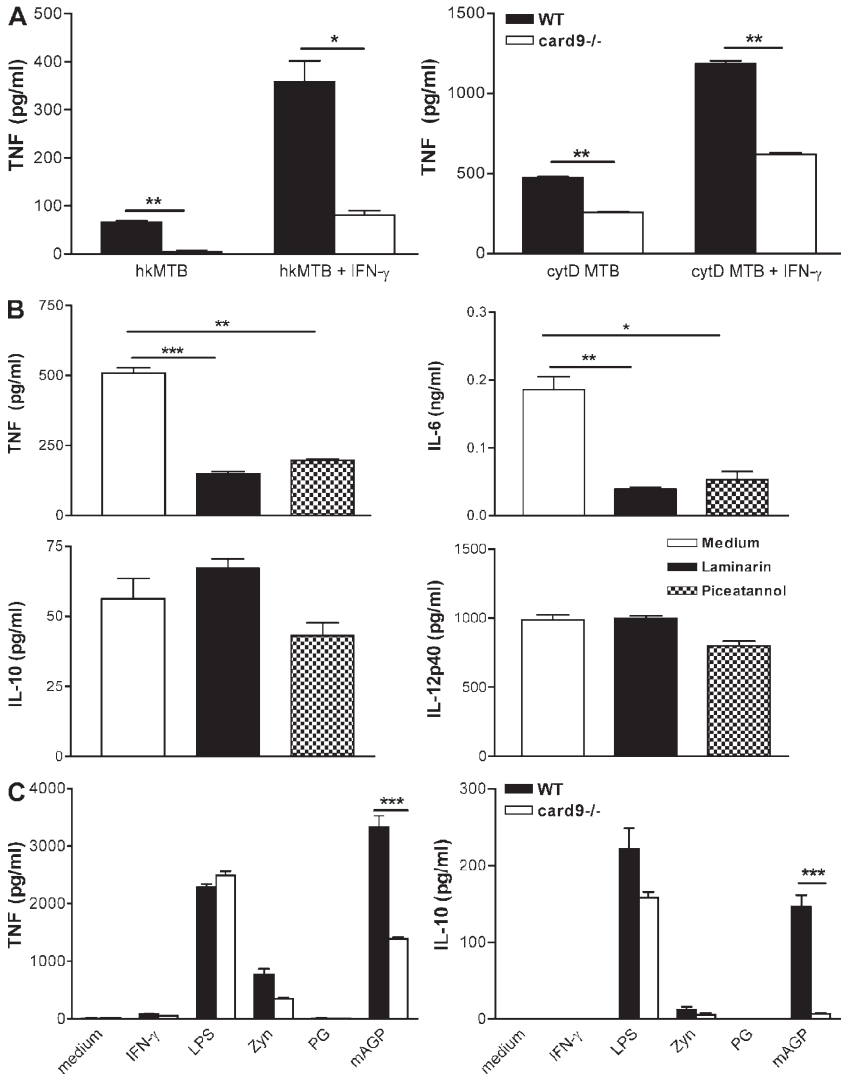

Figure 3. The adaptor molecule CARD9 converges signals from multiple PRRs involved in MTB recognition. (A) Deficient inflammatory cytokine production by *Card9*$^{-/-}$ BMDMs in response to heat-killed MTB or after blocking of phagocytosis. (B) Blocking dectin-1–syk pathway in WT cells recapitulated the observations reported for Card9$^{-/-}$ BMDMs, as revealed by selective impairment of TNF and IL-6 production. (C) mAGP induced diminished cytokine levels in *Card9*$^{-/-}$ macrophages. Data are mean ± SEM of two independent experiments with three replicates each. *, $P < 0.05$; **, $P < 0.01$; ***, $P < 0.001$, Student's *t* test.

and WT mice mounted similar delayed-type hypersensitivity (DTH) responses and protective immunity in response to BCG vaccination (Fig. 4, C and D). Thus, vaccination-induced acquired immunity overcame CARD9-dependent innate immune deficiency. We conclude that CARD9 defects affect innate immune rather then acquired T cell responses in TB.

The *Card9* deficiency caused marked accumulation of neutrophils in the lungs of infected mice (Fig. 5 A). The frequency of DCs and lung macrophages, as well as the expression level of a maturation marker expressed by APC (CD86), in infected lungs did not differ between the mouse strains (Fig. 5 B). Yet, myeloperoxidase (MPO) staining

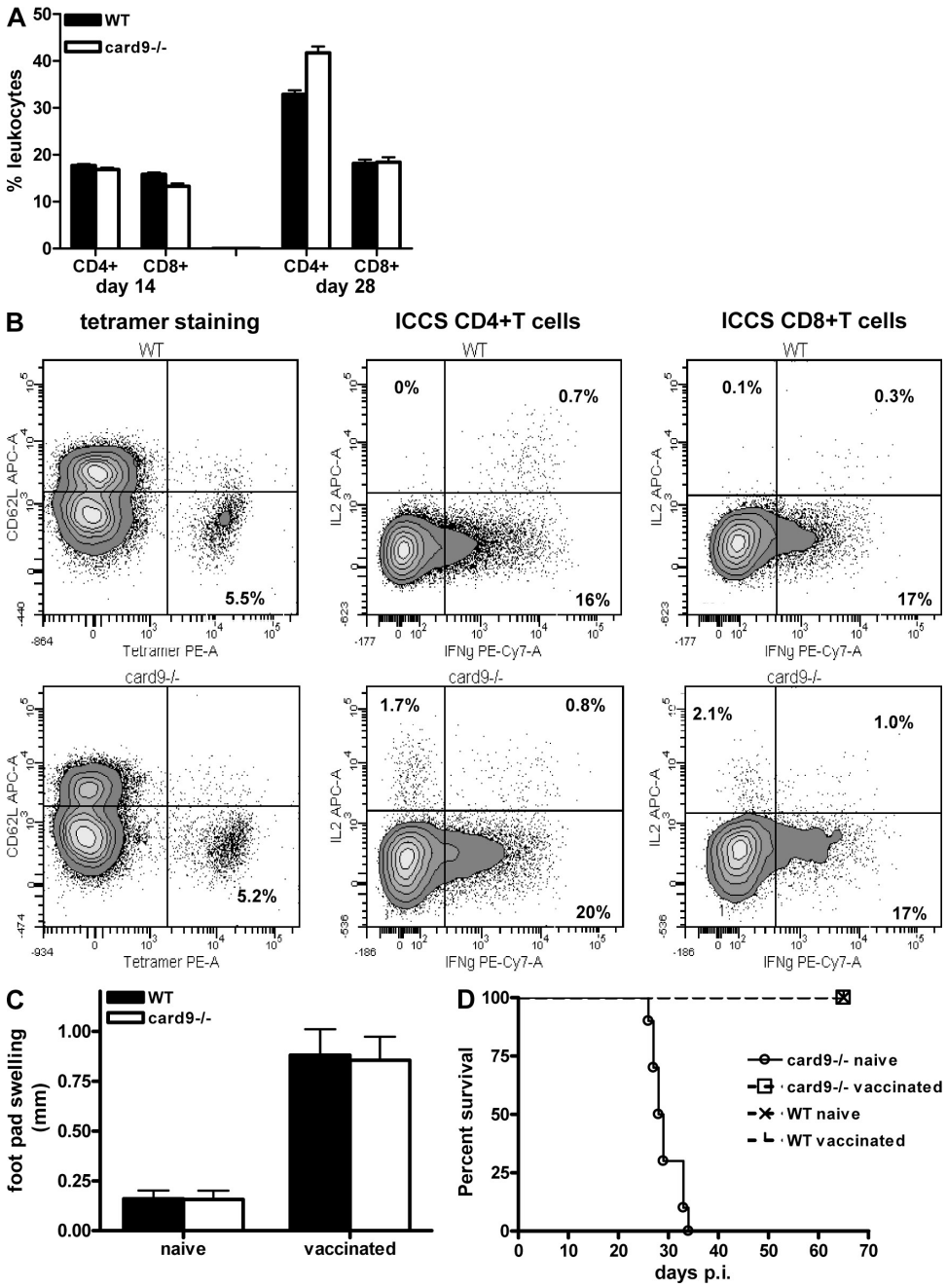

Figure 4. ***Card9*$^{-/-}$ mice develop efficient T cell responses to mycobacterial infections.** (A) Lymphocyte percentages were similar in MTB-infected *Card9*$^{-/-}$ and WT mice at 14 and 28 d p.i. as shown by FACS analysis of CD4$^+$ and CD8$^+$ lung T cell populations. (B) *Card9*$^{-/-}$ mice mounted normal lung T cell responses, as revealed by frequencies of MTB-specific PepA tetramer$^+$ (GAPINSATAM) CD8$^+$ T cells and IFN-γ/IL-2$^+$ CD4$^+$ or CD8$^+$ T cells. Data are representative of two independent experiments (n = 5). Two-way ANOVA and Bonferroni method were applied for statistical analyses. (C) WT and *Card9*$^{-/-}$ mice develop similar DTH responses 3 wk after BCG vaccination (n = 12). (D) Survival of *Card9*$^{-/-}$ mice challenged with 200 CFUs of MTB H37Rv is significantly prolonged by BCG vaccination (n = 10). Data shown is from one experiment (C and D).

demonstrated that granulocytes accumulated in nest-like structures within large inflammatory foci (Fig. 5 G). The accelerated lung recruitment of polymorphonuclear neutrophils (PMNs) was paralleled by aggravated disease, suggesting a critical role of neutrophils in disease progression to fatal outcome.

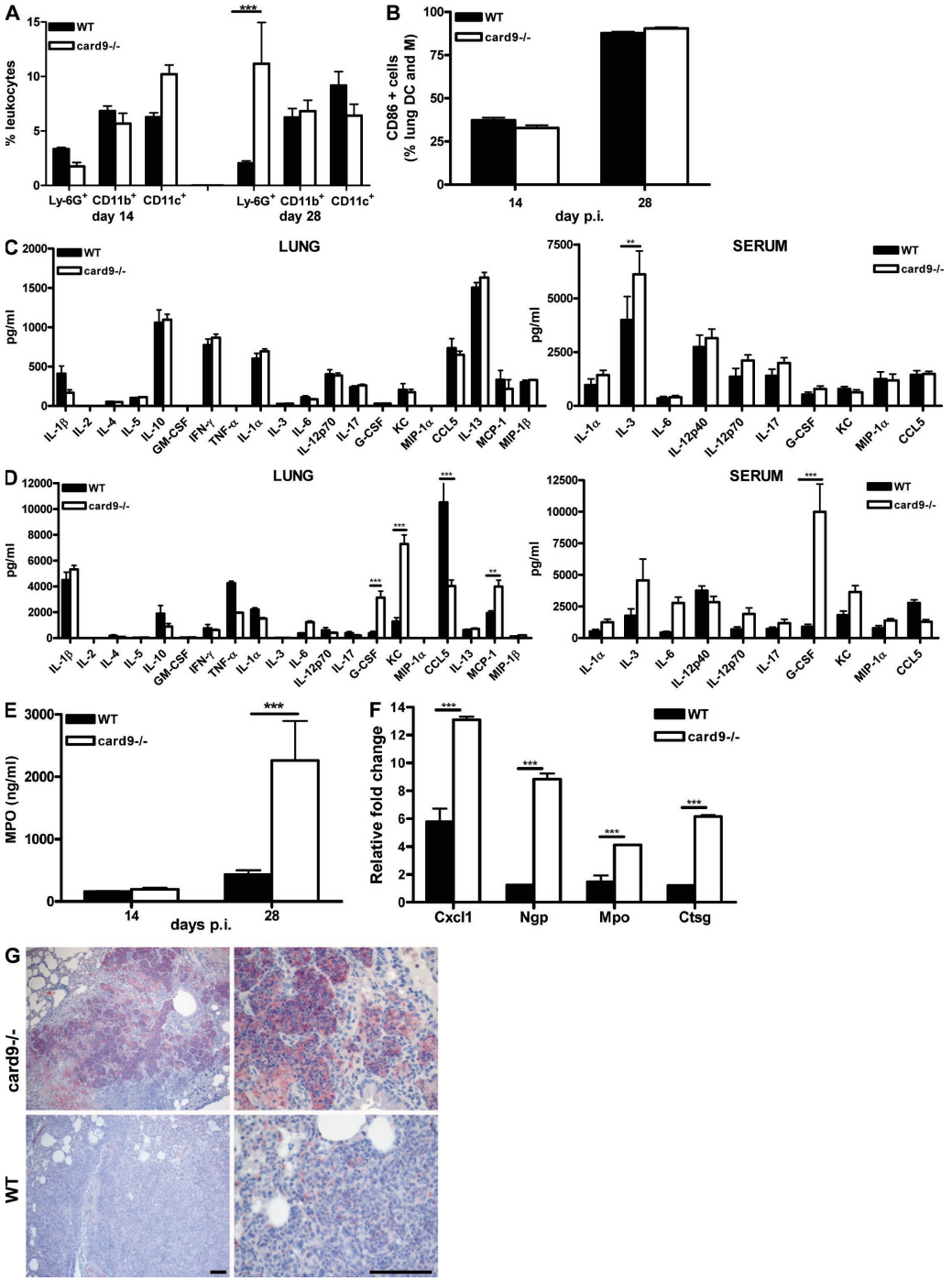

Figure 5. Susceptibility of *Card9*$^{-/-}$ mice to tuberculosis is caused by increased granulopoiesis and accelerated neutrophil recruitment to inflamed lungs. (A) Neutrophil accumulation in lungs during TB in *Card9*$^{-/-}$ mice and (B) expression of the costimulatory molecule CD86 on surface of lung DCs and macrophages. (C and D) Analysis of cytokine and chemokine concentrations in lung homogenates and sera revealed that *Card9*$^{-/-}$ mice developed systemic inflammatory responses with increased local proinflammatory cytokines and high levels of soluble mediators of granulocyte development and chemotaxis at day 14 p.i. (C) and day 24 p.i. (D). (E) Increased serum levels of granulocyte MPO in *Card9*$^{-/-}$ mice. (F) Up-regulation of PMN-related genes in lung of infected mice 14 d p.i. (G) *Card9*$^{-/-}$ mice presented multiple clusters of MPO^{+} granulocytes within large inflammatory lung infiltrates. Bar, 100 µm. Data are representative of two independent experiments ($n = 5$). Two-way ANOVA and Bonferroni method were applied for statistical analyses. **, $P < 0.01$; ***, $P < 0.001$.

We attempted to define triggers of neutrophilic inflammation during MTB infection and to verify the relevance of disbalanced cytokine responses as observed in vitro. To this end, we determined chemokine and cytokine concentrations in lung homogenates and serum. 2 wk p.i., we barely detected any differences (Fig. 5 C), but obvious changes appeared by 3 wk p.i. (Fig. 5 D). CCL5 concentration was reduced in the lungs of *Card9*$^{-/-}$ mice. This deficiency alone could not explain the heightened lethality of *Card9*$^{-/-}$ animals to TB because CCR5 has multiple ligands (including MIP-1α and MIP-1β) and there is substantial redundancy in the chemokine system (Algood and Flynn, 2004; Badewa et al., 2005). Strikingly, MCP-1 and cytokines involved in neutrophil differentiation (G-CSF) and recruitment (keritinocyte-derived chemokine [KC]) were markedly elevated in susceptible mice. Moreover, we detected increased concentrations of granulocyte-derived MPO in sera of *Card9*$^{-/-}$ mice (Fig. 5 E). In absence of CARD9, PMN transcriptional responses were detected as early as 14 d p.i., at a time-point where bacterial burdens did not differ (Fig. 5 F). Thus, we consider systemic inflammatory disease followed by tissue damage a result of augmented granulocyte differentiation in the BM by G-CSF and accelerated recruitment of these neutrophils to the lung by KC.

We interrogated whether adaptor deficiency in hematopoietic cells was the primary cause of uncontrolled inflammation and lethality. We generated *Card9*$^{-/-}$/WT bone-marrow chimera mice and challenged them with virulent MTB. Transfer of CARD9 KO cells into irradiated WT mice rendered recipients susceptible to TB, demonstrating a critical role of hematopoietic rather than radio-resistant cells in control of TB in absence of CARD9 (Fig. 6 A). Because of increased PMN recruitment to lungs of *Card9*$^{-/-}$ mice we compared expression of CARD9 in PMN versus other myeloid cells and alveolar epithelial cells (AECs). PMN abundantly expressed CARD9 transcripts in steady-state, whereas BMDCs and lung macrophages were similar in terms of adaptor transcriptional activity (Fig. 6 B). AECs showed negligible

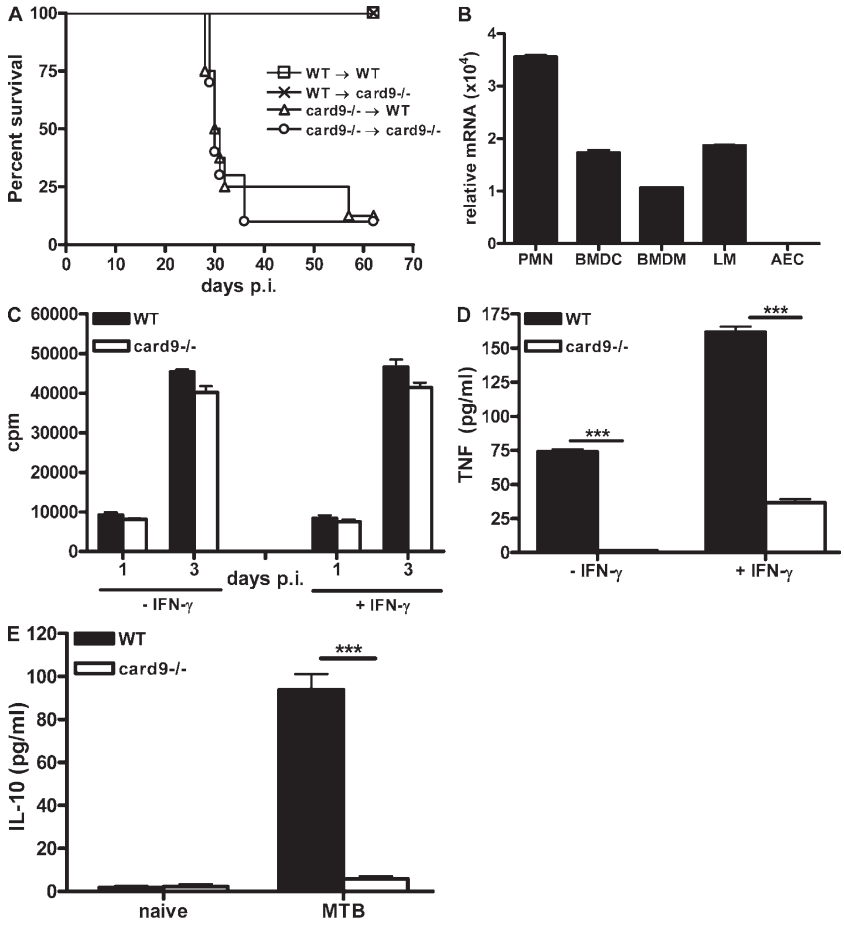

Figure 6. Susceptibility of *Card9*$^{-/-}$ mice to tuberculosis resides in the hematopoietic compartment and is linked to *Card9*$^{-/-}$ PMN deficiencies to produce both pro- and antiinflammatory cytokines during TB infection. (A) BM chimeras were infected with 200 CFUs of MTB H37Rv and survival was followed up for 65 d p.i. (n = 8–10). (B) CARD9 expression in myeloid cells and AECs. (C) PMN from WT and *Card9*$^{-/-}$ mice were infected with MTB H37Rv at MOI 5 and bacterial multiplication assed by [^{3}H]Uracil incorporation. TNF (D) and IL-10 (E) levels in supernatants of MTB-infected PMN, determined by ELISA (MOI 5). Data are mean ± SEM of two experiments with six replicates each (C) or are representative of four independent experiments with three to six replicates each (D and E). *, $P < 0.05$; **, $P < 0.01$; ***, $P < 0.001$, Student's t test.

transcriptional activity. After MTB encounter, CARD9$^{-/-}$ PMN released less TNF compared with WT controls, but apparently did not support mycobacterial growth (Fig. 6, C and D). PMN isolated from KO mice had lost their propensity to secrete IL-10 when challenged with MTB (Fig. 6 E). We conclude that CARD9-deficient animals fail to fine-tune lung inflammation by means of IL-10.

Both neutrophilic inflammation and MTB replication render *Card9*$^{-/-}$ mice susceptible to TB

To further assess whether neutrophilic hyperreactivity and subsequent tissue damage accounted for lethality of MTB infected *Card9*$^{-/-}$ mice, we designed rescue experiments. Two different strategies were followed. First, we used the cholesterol-lowering agent lovastatin to accelerate removal of apoptotic

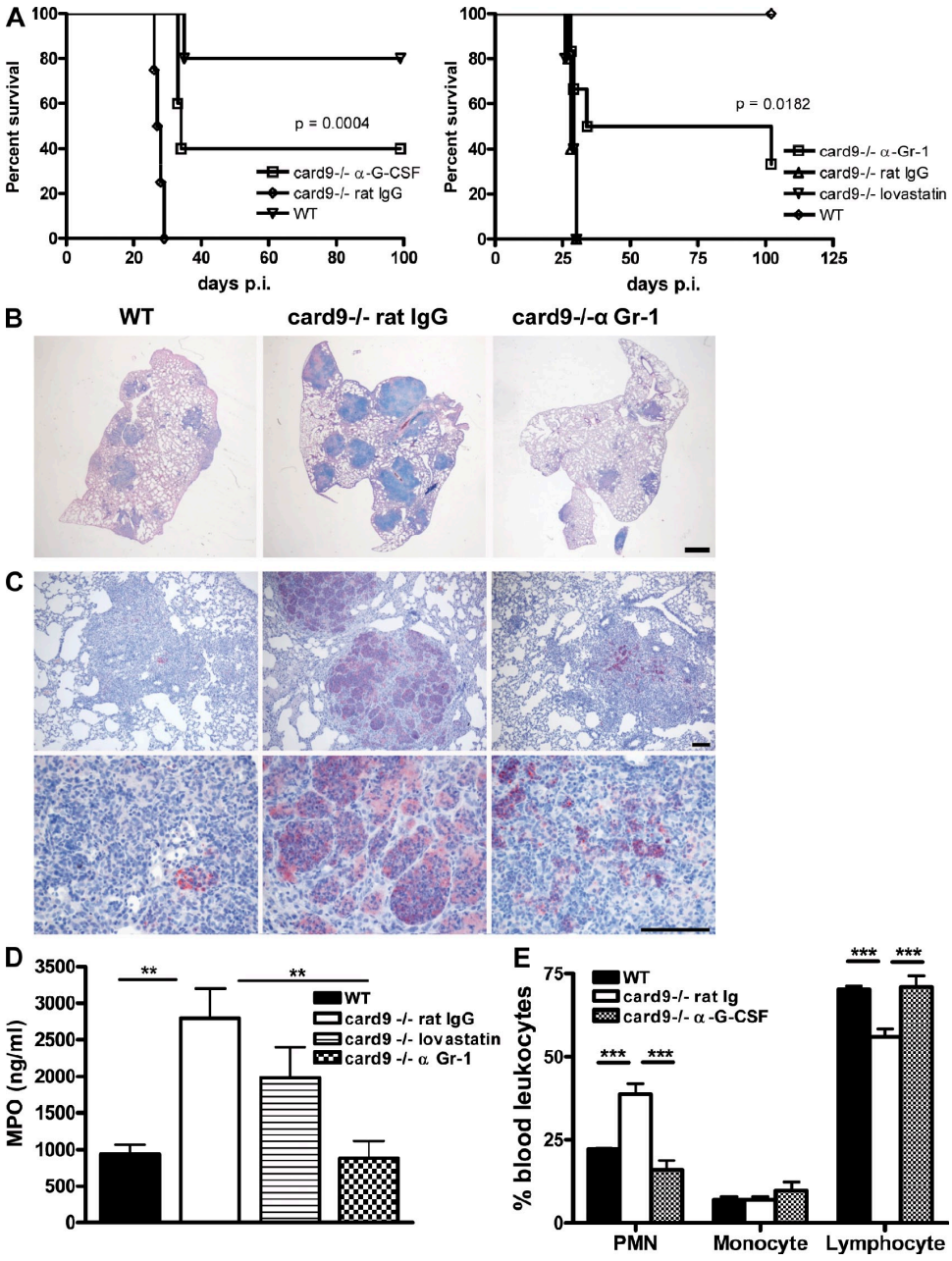

Figure 7. Neutrophil depletion ameliorates lung inflammation and prolongs survival. (A) Neutrophil depletion or G-CSF neutralization resulted in increased survival of MTB-infected *Card9*$^{-/-}$ mice, Kaplan-Meier curves, and log-rank test. (B) Giemsa staining of infected lungs 24 d p.i. showed that granulocyte depletion ameliorated lung inflammation. (C) PMN depletion limited parenchyma infiltration with MPO^{+} cells. (D) PMN depletion reduced circulating levels of MPO and (E) PMN numbers (n = 4–6). Data are representative of one (G-CSF) or two (Gr-1) independent experiments (n = 5–10; 24 and 21 d p.i., respectively). Two-way ANOVA and Bonferroni method were applied for statistical analyses. Bars: (B) 2.5 mm; (C) 100 µm. **, $P < 0.01$; ***, $P < 0.001$.

cells in the lung (Morimoto et al., 2006). Impaired removal of apoptotic cells causes secondary necrosis, thus triggering tissue damage (Kono and Rock, 2008). Second, we modulated inflammatory responses by either neutralizing G-CSF or depleting PMNs with anti Gr-1 monoclonal antibody (mAb). Treatment with lovastatin did not improve survival. In contrast, granulocyte-limiting approaches prolonged survival of MTB-infected *Card9*$^{-/-}$ mice (Fig. 7 A). Although bacterial burdens were not significantly altered after treatment at 21 (G-CSF neutralization, preliminary data) or 25 d p.i. (PMN depletion; Fig. S7), survival was prolonged and accompanied by ameliorated lung inflammation, in 60–70% of the treated animals, and fewer MPO-positive cells were recruited to the lungs (Fig. 7, B and C). Remarkably, both treatments reduced circulating levels of MPO and granulocytes (Fig. 7, D and E). Thus, limiting granulocyte infiltration of the lung dampened inflammation and prolonged survival of susceptible mice.

Next, we interrogated whether uncontrolled inflammation could be brought to an end by anti-TB therapy. In preliminary experiments, we used the first-line TB drugs isoniazid (INH) and rifampicin (RIF) to reduce bacterial burden (Fig. 8, A–C). Despite diminished susceptibility, there were 30% death cases during the first 10 d when chemotherapy was started 3 wk p.i. (Fig. 8 A). When drug treatment started 2 wk p.i., however, KO animals controlled TB infection (Fig. 8 D). MTB burdens in lung at the end of antibiotic treatment and 2 wk thereafter were more affected by INH/RIF in *Card9*$^{-/-}$ compared with WT mice (Fig. 8 E). We assume that reduced immune pressure in absence of CARD9 allowed for more metabolically active, replicating MTB with higher susceptibility to drug treatment. Collectively, mechanisms that fine-tune host inflammation and those controlling bacterial replication are both needed to overcome susceptibility to TB in the absence of CARD9.

DISCUSSION

The first events after MTB has reached the alveolar space of the host lung include its recognition by alveolar macrophages via PRRs. They recruit adaptor molecules that transduce

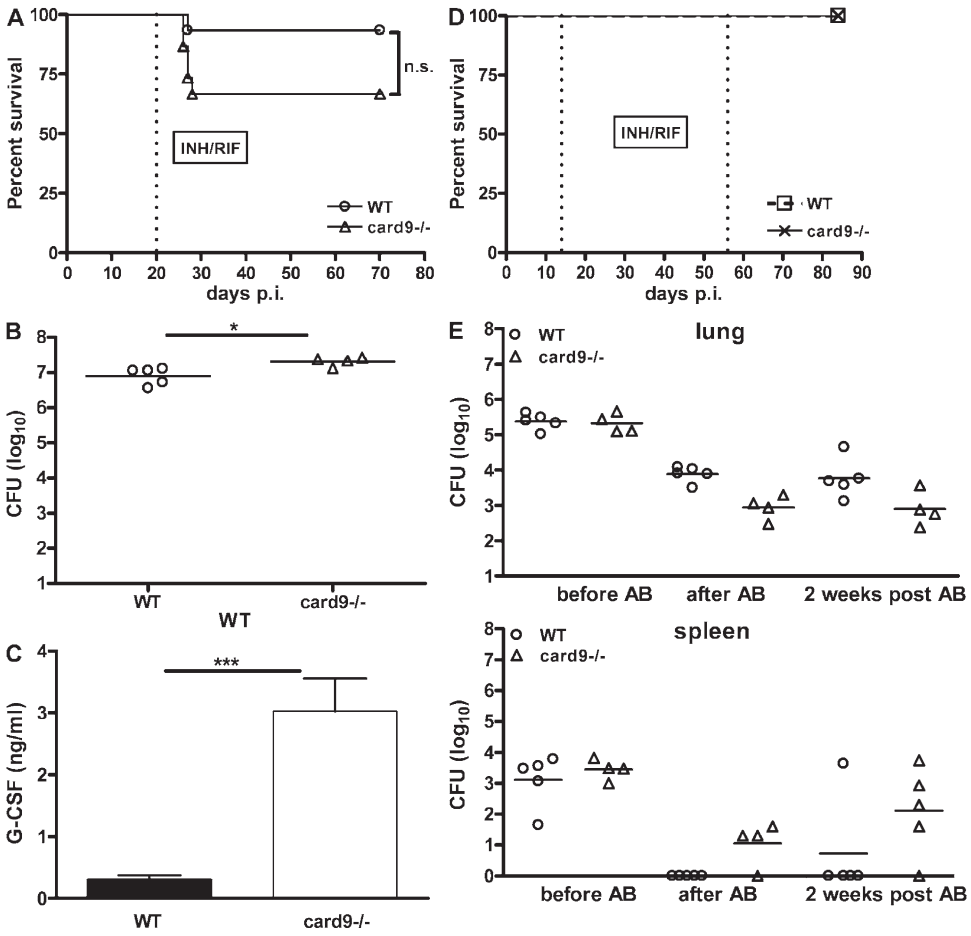

Figure 8. TB chemotherapy prolongs survival of *Card9*$^{-/-}$ mice. (A) Survival of mice infected with 400 CFUs MTB H37Rv and treated with INH/RIF (AB) at 3 wk p.i. Lung bacterial burdens (B) and serum G-CSF levels (C) at AB begin. (D) Survival of mice infected with 400 CFUs MTB H37Rv and treated with AB at 2 wk p.i. (E) MTB burdens in lungs and spleens of WT and KO mice before and after AB treatment. Data from one (A–C; $n = 15$) or two experiments (D and E; $n = 15$). Mann-Whitney test was applied for statistical analyses, for survival Kaplan-Meier curves were used. *, $P < 0.05$; ***, $P < 0.001$.

signals culminating in transcriptional responses that determine the type of the ensuing immune response. The adaptor molecule CARD9 is expressed in myeloid cells (Bertin et al., 2000) and in lung tissue (Hsu et al., 2007). Here, we demonstrate that: (a) CARD9 adaptor was central for sampling of signals from various PRRs involved in MTB recognition; (b) CARD9 was essential for control of pulmonary TB; (c) uncontrolled MTB replication and excessive lung inflammation resulted in lethal outcome of MTB infection in *Card9*$^{-/-}$ mice. We conclude that CARD9-dependent tight control of, and by, PMN are essential for innate immunity in TB. Our data thus emphasize the double-edged role of innate immunity in protection and pathology in TB.

Disruption of TLRs impairs long-term control of TB (Hölscher et al., 2008) and deficiencies in IL-1R (Fremond et al., 2007), MyD88 (Fremond et al., 2004), or TIR8 (Garlanda et al., 2007) result in fatal acute TB disease. Animals devoid of TIR8, a negative regulator of TLR signaling, or D6, a decoy and scavenger receptor for inflammatory CC chemokines, suffer from uncontrolled systemic inflammation, although they normally control bacterial replication (Garlanda et al., 2007; Di Liberto et al., 2008). These findings indicate that control of both bacterial growth and inflammation are decisive determinants of disease outcome. MTB-infected *Card9*$^{-/-}$ mice suffered concomitantly from higher MTB burdens in lungs and a systemic inflammatory response associated with profound lung pathology. Pyogenic pneumonia in *Card9*$^{-/-}$ mice resembled lesions observed in MTB-infected MyD88 and IL-1R KO mice (Fremond et al., 2004, 2007) or mice deficient for *Ipr1* gene within the *sst1* locus (Pan et al., 2005). Despite excessive cell death in the lung, *Card9*$^{-/-}$ BMDMs were equally prone to apoptosis as their WT counterparts in contrast to the sst1-susceptible macrophages (Pan et al., 2005), suggesting that CARD9 is not directly involved in apoptosis control. In infected *Card9*$^{-/-}$ mice, increased apoptosis in lungs was not compensated by cellular replacement, similar to some extent to mice deficient in the IL-1–MyD88 pathway (Fremond et al., 2004, 2007).

Deficient IL-1 signaling accounts for most of the MyD88 KO phenotype because of a shared signaling pathway (Fremond et al., 2007). CARD9 does not share any molecules involved in signal transduction with either IL-1R or the MyD88 adaptor, but regulates IL-1β release at APC level. Its propensity to regulate inflammasome function was recently revealed during fungal infection (Gross et al., 2009). Accordingly, we exclude a major impact of MyD88 on CARD9 signaling. Instead, we consider more likely a regulatory loop via modulation of IL-1β release by CARD9 signaling. Consistent with our assumptions, sensing of MTB by dectin-1 and NOD2 is MyD88-independent. Our in vitro data point to a syk dependency of dectin-1 signaling, whereas NOD2 signaling involves stable ubiquitination of RIP2 (Yang et al., 2007). *Card9*$^{-/-}$ mice up-regulated iNOS in inflamed lungs and *Card9*$^{-/-}$ BMDMs controlled MTB growth in vitro and produced NO similar to WT cells. Moreover, LRG-47 expression after MTB infection was apparently not impaired in *Card9*$^{-/-}$ mice (Fig. S8). Thus, increased susceptibility of *Card9*$^{-/-}$ mice was not caused by defective production of these antimicrobial effector molecules. Yet, CARD9 was required for an efficient innate activation program in vitro and for antimycobacterial immune homeostasis in vivo. We observed reduced cytokine synthesis by KO cells after MTB encounter. Reduced TNF production could explain defective granuloma formation, at least in part (Bean et al., 1999; Chakravarty et al., 2008). Diminished IL-12 synthesis by macrophages was reproduced in DCs, but could not be detected in infected tissue. Because of similar lung levels of IL-12, critical for Th cell polarization (Khader et al., 2006), apparently unrestrained Th1 responses could develop in absence of CARD9 signaling during TB. *Card9*$^{-/-}$ mice suffered from higher bacterial titers as early as 3 wk p.i. In parallel, the animals exhibited pyogranulomatous infiltrates rich in neutrophils in the lung, increased death, and impaired removal of dead cells from the lung parenchyma. Fatal disease progression in the absence of CARD9 signaling was thus accompanied by exacerbated inflammation induced by granulocytes.

The relevance of PRRs for initiating and shaping adaptive immunity is beyond doubt (Medzhitov, 2007; Dorhoi and Kaufmann, 2009). Strikingly, absent CARD9 signaling did not seem to affect T cell responses to MTB, suggesting it is dispensable for development of appropriate T cell responses in TB. *Card9*$^{-/-}$ mice developed normal Th1 responses to MTB in vivo despite reduced IL-12 production by APC in vitro. Moreover, we did not detect any deficiency in Th17 response to MTB, although involvement of the syk-CARD9 pathway in differentiation of IL-17-producing CD4^{+} T cells has been described (LeibundGut-Landmann et al., 2007). Neutrophil-mediated defense against *C. albicans* induced by efficient Th17 responses is CARD9 dependent. Mycobacteria are decorated with various pathogen-associated molecular patterns that trigger multiple PRRs simultaneously, whereas *C. albicans* is rich in β-glucans, which are sensed by CLRs. Simultaneous engagement of an array of PRRs likely has a different outcome (Seimon et al., 2006; Trinchieri and Sher, 2007). Hence, multiple receptor recognition of MTB cannot be mimicked by single receptor–ligand interactions, such as synthetic TDM derivatives. Our Th17 data during MTB infection are consistent with a recent study by Werninghaus et al. (2009), although the two studies investigated different tissue sites. The differences in IFN-γ producers in the lung tissue was not confirmed in our study, although overall lung IFN-γ abundance did not differ (Fig. 5, C and D). Notably, both studies point to efficient T cell activation in absence of CARD9. Strikingly, despite using a similar dose of MTB laboratory strain, the CARD9 KO animals survived longer in this study (Werninghaus et al., 2009). This could be explained by differential virulence of the MTB stocks used. In any case intact T cell immunity failed to overcome the severe innate defects of *Card9*$^{-/-}$ mice in MTB infection. On the contrary, protective T cell responses were efficiently stimulated by BCG vaccination. CARD9 KO mice not only developed DTH, but also protection against MTB. We conclude that in the

absence of CARD9, innate inflammation cannot be controlled although apparently adequate T cell responses can develop.

MTB recognition by different TLRs (Quesniaux et al., 2004; Schnappinger et al., 2006) and NOD2 (Ferwerda et al., 2005; Gandotra et al., 2007; Yang et al., 2007) is well established. Moreover, evidence for a role of CLRs in MTB sensing has been obtained (Yadav and Schorey, 2006; Rothfuchs et al., 2007). The complexity of the MTB cell wall requires combinatorial recognition and engagement of different types of PRRs, as emphasized by our experiments. Further, our data establish a critical involvement of CARD9 signaling in cytokine secretion by BMDMs in response to MTB and evidence that MTB sensed by dectin-1 and NOD2 uses CARD9 as an adaptor molecule. Involvement of other ITAM-based molecules that signal via CARD9, including Mincle, a CLR member recently proposed to sense mycobacterial TDM (Ishikawa et al., 2009), cannot be excluded. Convergence of multiple PRR pathways on the CARD9 adaptor minimizes metabolic expenses for the host. On the other hand, convergence increases host vulnerability. Consistent with recent gene expression profiling results, demonstrating that CARD9 is modulated in human DCs early after MTB infection (Tailleux et al., 2008), our data emphasize the need to clarify whether polymorphisms in CARD9 influence susceptibility to MTB in humans. Recent genetic analysis extended the link between fungi detection and CARD9 signaling from the mouse to the human system. Homozygous CARD9 mutation was found to predispose humans to chronic mucocutaneous candidiasis (Glocker et al., 2009). Based on our observations in TB-infected naive and BCG-vaccinated *Card9*$^{-/-}$ mice, and because of the fact that in TB-endemic regions vaccination programs are in place, genetic screening for an association between CARD9 polymorphisms and susceptibility to TB is challenging but necessary.

Lung damage in *Card9*$^{-/-}$ mice was governed by augmented granulopoiesis, neutrophilic inflammation, and apoptotic cell death which progressed to secondary necrosis. Pathology was correlated with local production of G-CSF, KC, and MCP-1 and systemic release of G-CSF. These cytokines are produced by myeloid, endothelial, and epithelial cells and stimulate granulopoiesis and attract granulocytes to tissue sites. G-CSF is induced by various cytokines and bacterial products and stimulates differentiation, maturation, and functional activation of neutrophilic granulocytes. Evidence is accumulating that acute mobilization of PMNs from the BM is induced by simultaneous release and action of G-CSF and KC (Wengner et al., 2008). This cytokine millieu occurred in TB-infected mice in absence of CARD9 and induced both release of granulocytes into the periphery and their accelerated recruitment to the lung. Transcriptional regulation of KC was augmented early after infection and paralleled PMN-specific transcripts. Neutrophil-specific genes are actively transcribed during differentiation in BM under steady-state conditions (Borregaard et al., 2007). However, during infectious stress and high neutrophil demand immature granulocytes are released, and hence PMN transcripts can be detected in infected tissue sites. Recent studies revealed that granulopoietic emergency program depends on IL-1R signaling and that low IL-1β levels could induce late neutrophilic responses (Ueda et al., 2009). Although we did not detect significant in vivo IL-1β differences between the CARD9 KO mutants and congenic controls during TB, the potential role of the CARD9 adaptor in hematopoetic stem cell and progenitor proliferation remains to be established. *Card9* deficiency reduces nuclear translocation of NF-κB (Gross et al., 2006), and KC comprises NF-κB–binding sites in its promoter (De Filippo et al., 2008). Reduced proinflammatory cytokine responses in MTB-infected macrophages in vitro support deregulated KC synthesis. Diminished IL-6 production could directly impair KC abundance because gp130-dependent STAT-3 signaling negatively regulates KC responses and PMN clearance (Fielding et al., 2008). Whether lung PMN kinetics is directly affected or whether the emergency granulopoietic program is distorted remains to be clarified. Beneficial effects of PMN depletion or G-CSF neutralization support pathological functions of the granulocytes during acute TB in the absence of CARD9. Importantly, previous studies on transient PMN depletion by anti–Gr-1 mAb in WT mice (Seiler et al., 2000; Keller et al., 2006) did not observe major effects on TB, as seen here for CARD9 KO mutants (Fig. 7 A). Although inflammatory monocytes are Gr-1^{+} (Geissmann et al., 2003) and mAb treatment could have affected this population, available data rule out a major involvement of these cells in TB. Mice deleted in CCL2 (Kipnis et al., 2003) or CCR2 (Scott and Flynn, 2002), which are required for tissue recruitment or egress from BM of inflammatory monocytes, respectively, controlled MTB infection efficiently. We conclude that exacerbated lung neutrophilic inflammation represents a hallmark of lung pathology in MTB-infected *Card9*$^{-/-}$ mice. Although PMN depletion reduced inflammation and prolonged survival, it did not considerably impact on bacterial burdens in lung, suggesting that inflammation alone triggered lethality. However, reduction of MTB loads by drug treatment during polarized PMN inflammation rescued *Card9*$^{-/-}$ mice from lethal outcome.

The role of neutrophils in TB remains controversial (Seiler et al., 2000; Eruslanov et al., 2005; Keller et al., 2006). Our data reveal that PMN abundantly transcribe CARD9, yet reveal a detrimental role of granulocytes in TB. Our observation is consistent with a recent study describing a previously unknown role of PMN in dampening inflammation via IL-10 (Zhang et al., 2009). We demonstrate that CARD9 is essential for IL-10 synthesis in MTB-infected PMN. Absent IL-10 in CARD9 KO animals abrogated negative feedback regulation of various cytokine and chemokine genes. Control by both MyD88 and CARD9 of IL-10 production in PMN during TB could explain the similar pathology of MTB-infected KO mice deficient in CARD9 or MyD88. Neutrophilic inflammation of the lung is followed by defective removal of apoptotic cells, termed efferocytosis. Studies on chronic lung inflammation emphasize an important role of early efferocytosis for maintenance of biological lung functions

(Vandivier et al., 2002). Moreover, a detrimental role of so-called "frustrated" PMN, unable to meet the pathogen in inflamed tissue, has been described (Nathan, 1987). In MTB-infected *Card9*$^{-/-}$ mice, collateral damage during secondary necrosis and systemic release of MPO became life threatening. Neutrophils undergoing necrosis leak enzymes and noxious agents that damage the surrounding tissue without contributing to MTB control. Notably, granulocyte-derived MPO causes cytotoxicity in alveolar macrophages (Grattendick et al., 2002). Increased levels of circulating MPO were recently reported in patients with active lung TB (Koziol-Montewka et al., 2004). As a corollary, we assume absence of a regulatory loop via lack of IL-10 and a circulus vitiosus with granulocytes initiating inflammation and ineffective efferocytosis boosting inflammatory responses. Collectively, we conclude that both fine-tuning of acute PMN inflammation and control of MTB replication in lung tissue are responsible for lethal TB in absence of CARD9 signaling. The molecular mechanisms underlying unleashed bacterial growth remain to be deciphered. Susceptibility is apparently independent from control by the acquired T cell response and can be overcome by vaccination. Thus, the key adaptor CARD9 plays an essential role in autonomous orchestration of innate immunity in TB.

MATERIALS AND METHODS

Antibodies and chemical reagents. The following polyclonal antibodies were used for immunostainings: MPO (Abcam), iNOS (LabVision), and goat anti–rabbit (Dianova). We used the following mAb for flow cytometric investigations: CD4 (RM4-5), IFN-γ (XMG-1.2), IL-2 (JES6-5H4), Ly6G/C (RB6-8C5), CD11b (M1/70; eBioscience), CD8α (YTS169), TNF (XT22), CD3 (145-2C11), CD28 (37.51), CD62L (MEL-14), CD25 (PC61), CD16/CD32 (2.4G2), F4/80 (CI:A3-1), and CD11c (N418; antibodies purified from hybridoma supernatants; American Type Culture Collection), IL-17 (TC11-18H10; BD Biosciences). PG, mAGP, AG, MAME, and manLam were derived from MTB (Colorado State University). LPS and zymosan were obtained from Invivogen; piceatannol and lovastatin were obtained from Calbiochem; TDM, cytochalasin, and laminarin were obtained from Sigma-Aldrich. DNaseI and collagenase D were obtained from Roche. CD11c beads were used for selection of differentiated BMDCs (Miltenyi Biotec).

Mice and MTB infection. WT (C57BL/6) and *Card9*$^{-/-}$ mice (Gross et al., 2006) were bred at III. Medizinische Klinik, Klinikum rechts der Isar, Technische Universität München, Germany. The *Card9*$^{-/-}$ mouse strain was backcrossed onto the genetic background of C57BL/6 for more than six generations. Mice were 8–12 wk of age at the beginning of the experiments, matched for age and sex, and kept under specific pathogen-free (SPF) conditions at the Max Planck Institute for Infection Biology in Berlin, Germany. Infection of mice was performed using a Glas-Col inhalation exposure system. The initial challenge dose was verified 24 h p.i. by plating complete lung homogenates onto Middlebrook 7H11 agar plates. At different time points, bacterial burdens were assessed by mechanical disruption of the organs in water/1% wt/vol BSA/1% vol/vol Tween 80 (WTA), and plating serial dilutions onto Middlebrook 7H11 agar plates. After 3 wk, MTB colonies were counted. For PMN depletion, mice were treated i.p. with anti-Gr-1 antibodies (Rb6-8C5) in PBS 200 μg/mouse/shot or with control rat IgG at days 8, 11, and 14 p.i. G-CSF neutralization was achieved by i.p. injection of 100 μg/mouse/shot anti–mouse G-CSF (R&D Systems) at days 10 and 14 p.i. Mice were treated with first-line TB drugs INH (0.1 g/liter) and RIF (0.1 g/liter; Fluka) in drinking water for 6 wk. Antibiotic treatment started at different time points p.i., as indicated in text or figure legend. Animal protocols were approved by Landesamt für Gesundheit und Soziales, Berlin, Germany.

BCG vaccination and DTH. Mice were s.c. inoculated with 10^6 CFUs BCG Danish 1331 (SSI). At 3 wk after vaccination, BCG-vaccinated and control mice were i.d. challenged with 2 μg PPD into the footpad (SSI). Foot pad swelling was recorded 48 h after challenge using a dial gauge caliper.

BM chimera generation and infection. WT and *Card9*$^{-/-}$ mice at 8 wk of age were maintained on antibiotics (0.1 mg/ml Ciprofloxacin and 2 mg/ml Neomicin) 1 wk before irradiation. Irradiation was performed using a dose of 4 Gy, and animals were further kept for 4 wk on antibiotics in drinking water. After withdrawal of antibiotics, complete repopulation of the organs with immune cells was allowed for another 4 wk, and, subsequently, leukocytes were PCR typed to control efficacy of reconstitution. MTB aerosol infection was performed (as described in the Mice and MTB infection section) at 10 wk after sublethal whole-body irradiation and complete reconstitution with donor leukocytes.

Primary cell cultures and innate immunity assays. BMDMs and BM-DCs were obtained from tibia and femur bones and maintained in Dulbecco's Modified Eagle Medium containing 20% L929-cell supernatant, 10% heat-inactivated FCS, 5% heat-inactivated HS, 2 mM glutamine or RPMI supplemented with 10% heat-inactivated FCS and 200 U/ml recombinant mouse GM-CSF, respectively. Differentiated resting cells and cells pretreated with recombinant mouse IFN-γ (100 U/ml; Strathmann Biotech AG) were infected with MTB H37Rv at MOI 5 or treated with MTB-derived compounds. MTB-derived compounds were solubilized in PBS unless otherwise stated. PG and mAGP were sonified for better solubilization. TDM solution was prepared by repeatedly warming the solution in PBS containing 2% DMSO at 50°C, followed by repeated vortexing. PMN were isolated from BM as previously described (Allport et al., 2002). For in vitro infection experiments, MTB was grown in Middlebrook 7H9 broth (BD) supplemented with 0.05% glycerol and Tween 80, and 10% ADC enrichment (BD) to an early log phase and washed with PBS, and single bacteria were resuspended in culture media at desired concentrations. After a 4-h incubation, noninternalized bacteria were washed away and incubation continued as indicated in the results. For blocking experiments, we used laminarin (500 μg/ml) and piceatanol (1–10 μM). MTB was heat inactivated at 80°C for 40 min. Bacterial growth was assessed by [^{3}H]Uracil incorporation (Flesch and Kaufmann, 1987). Concentration of TNF, IL-6, CCL5, IL-10, and IL-12p40 in cell culture supernatants was determined 24 h p.i. or after stimulation using commercial ELISA kits (R&D Systems). Apoptotic rates were measured using Cell Death Plus Detection kit ELISA (Roche) according to the manufacturer's instructions. Nitric oxide was determined using the Griess reagent (Sigma-Aldrich).

Multiplex cytokine assays. Sera and lung homogenates from MTB-infected mice were assayed for cytokine and chemokine levels using multiplex bead-based immunoassay kits (Bio-Plex Cytokine Assay; Bio-Rad Laboratories) according to manufacturer's instructions.

Quantitative RT-PCR. Lung tissue or, alternatively, cell pellets were homogenized in Trizol and mRNA was extracted using acidic phenol chloroform extraction. RNA integrity and the absolute amount of total RNA were verified with a Bioanalyzer 2100 (Agilent Technologies). Expression levels of Cxcl1, Ngp, Mpo, Ctsg, Irgm1, LRG-47, Card9, and housekeeping gene GAPDH were analyzed using QuantiTect primer-probes (QIAGEN). Fold changes were calculated with the ΔCT method using uninfected samples as calibrator for tissue analysis or normalized to GAPDH with the equation $1.8^{(\text{GAPDH-CARD9})} \times (1{,}000{,}000)$ to evaluate CARD9 expression in different cell types.

MPO concentration. Enzyme levels in sera from MTB-infected mice were determined using a commercial ELISA, according to manufacturer's instructions (Hycult Biotechnology).

Histology and immunohistochemistry. Organs were fixed with 4% wt/vol PFA for 24 h and embedded in paraffin. Sections (2 μm) were Giemsa stained. Mycobacteria in the lungs were visualized by acid-fast staining

(TB Stain kit; BD) according to manufacturer's instructions. For immunohistochemistry, fixed and rehydrated tissue sections were subjected to antigen retrieval, blocking and exposed to primary antibody, followed by goat anti–rabbit AP secondary antibody. Alkaline phosphatase activity was visualized using fuchsin (Dako). Sections were counterstained with hematoxylin. TUNEL staining was performed according to the vendor's protocol (in situ detection kit TMRed; Roche).

Flow cytometric analysis of lung and spleen cells. Purification of cells from lungs and spleens of MTB-infected mice was performed as previously described (Kursar et al., 2007). APC/phagocyte influx to lungs was assed by measuring frequencies of cells positive for the following markers: CD-11b, Ly6G, CD-11c. FoxP3$^+$ T cell frequencies were measured using the Foxp3 Staining Set (eBioscience). For intracellular cytokine staining (ICCS) cells were stimulated with polyclonal activators (anti-CD3/CD28 antibodies) or a pool of MTB-derived peptides ($Ag85A_{241\text{-}260}$ [QDAYNAGGGHNGVFDFPDSG], $Ag85B_{240\text{-}260}$ [FQDAYNAAGGHNAVFNFPPNG], $Ag85A_{261\text{-}280}$ [THSWEYWGAQLNAMKPDLQ], $TB10.4_{4\text{-}12}$ [IMYNYPAML], $ESAT6_{1\text{-}20}$ [MTEQQWNFAGIEAAASAIQG], and $Mtb32/RV0125_{309\text{-}318}$ [GAPINSATAM]). All peptides were obtained from JPT Peptide Technologies and used at 5×10^{-5} M concentration for 6 h in the presence of 25 μg/ml brefeldin A. Nonspecific background activation was determined by culturing cells in RPMI only. After washing and blocking unspecific antibody binding, we performed surface staining for CD8α, CD4, and intracellular staining for the following cytokines: TNF, IL-17, IL-2, and IFN-γ. Cells were analyzed using a FACSCanto II flow cytometer and FACSDiva software (BD).

PMN isolation from buffy coats and PMN uptake assay. PMN were isolated from buffy coats using the reversal method. Ficoll gradient separation was followed by Dextran sedimentation and osmotic lysis of remaining erythrocytes. Overnight apoptotic PMNs were co-cultured with BMDMs at a ratio 5:1 for 1 h. BMDM monolayers were washed extensively with PBS and fixed with 2.5% glutaraldehyde. Internalized apoptotic PMNs were visualized by adding MPO substrate o-dianisidine (Sigma-Aldrich) and microscopic examination.

GFP bacteria uptake. GFP-expressing BCG microorganisms were grown in Middlebrook 7H9 broth supplemented with glycerol and 0.05% Tween 80, and 10% ADC enrichment medium to an early log phase, washed in PBS, and single bacteria were resuspended in culture media at desired concentrations. Differentiated BMDMs and BMDCs were incubated at different MOI with fluorescent bacteria for 2 h. Cells were washed extensively with PBS, detached and stained for specific cell markers. APCs were analyzed using a FACSCanto flow cytometer and FACSDiva software.

Statistical analysis. PRISM GraphPad software was used for statistical analysis. Bacterial titers were analyzed by the Mann-Whitney test, survival was assessed by Kaplan-Meier curves and log-rank test. Frequencies and numbers of APC, cytokine-positive T cells, concentrations of cytokines and chemokines were compared using a two-way ANOVA followed by Bonferoni's post-test. In vitro cytokine levels were compared using t-student test. Only P values ≤ 0.05 were considered statistically significant.

Online supplemental material. Fig. S1 shows that *Card9*$^{-/-}$ mice gradually lost body weight during acute TB infection. Fig. S2 depicts spleen pathology and indicates that despite increased susceptibility to TB, *Card9*$^{-/-}$ mice had serum NO levels comparable to WT controls. Fig. S3 shows apoptotic PMN clearance capacities of *Card9*$^{-/-}$ and WT macrophages. Fig. S4 indicates impaired cytokine production in MTB-infected BMDCs from *Card9*$^{-/-}$ mice. Fig. S5 shows that laminarin treatment did not interfere with mycobacterial uptake and indicates that *Card9*$^{-/-}$ BMDMs and DCs were impaired in mAGP detection. Fig. S6 shows that *Card9*$^{-/-}$ mice mounted apparently intact T cell responses after TB challenge. Fig. S7 indicates that PMN depletion did not impact on bacterial burdens, but improved clinical disease. Fig. S8 shows that *Card9*$^{-/-}$ mice were not impaired in LRG-47 regulation in the lung during TB infection. Online supplemental material is available at http://www.jem.org/cgi/content/full/jem.20090067/DC1.

We thank M.L. Grossman and Diane Schad for help in preparing the manuscript. MTB-derived PG, mAGP, MAME, and AG were received as part of National Institutes of Health, National Institute of Allergy and Infectious Disease contract no. HHSN266200400091C, entitled "Tuberculosis Vaccine Testing and Research Materials," which was awarded to Colorado State University.

This work received financial support from the German Federal Ministry of Education and Research (Bundesministerium für Bildung und Forschung) Kompetenznetzwerk "PathoGenoMikPlus" to S.H.E. Kaufmann.

The authors have no conflicting financial interests.

Submitted: 8 January 2009
Accepted: 18 February 2010

REFERENCES

Algood, H.M., and J.L. Flynn. 2004. CCR5-deficient mice control *Mycobacterium tuberculosis* infection despite increased pulmonary lymphocytic infiltration. *J. Immunol.* 173:3287–3296.

Allport, J.R., Y.C. Lim, J.M. Shipley, R.M. Senior, S.D. Shapiro, N. Matsuyoshi, D. Vestweber, and F.W. Luscinskas. 2002. Neutrophils from MMP-9- or neutrophil elastase-deficient mice show no defect in transendothelial migration under flow in vitro. *J. Leukoc. Biol.* 71:821–828.

Badewa, A.P., L.J. Quinton, J.E. Shellito, and C.M. Mason. 2005. Chemokine receptor 5 and its ligands in the immune response to murine tuberculosis. *Tuberculosis (Edinb.).* 85:185–195. doi:10.1016/j.tube.2004.10.003

Bean, A.G., D.R. Roach, H. Briscoe, M.P. France, H. Korner, J.D. Sedgwick, and W.J. Britton. 1999. Structural deficiencies in granuloma formation in TNF gene-targeted mice underlie the heightened susceptibility to aerosol *Mycobacterium tuberculosis* infection, which is not compensated for by lymphotoxin. *J. Immunol.* 162:3504–3511.

Bertin, J., Y. Guo, L. Wang, S.M. Srinivasula, M.D. Jacobson, J.L. Poyet, S. Merriam, M.Q. Du, M.J. Dyer, K.E. Robison, et al. 2000. CARD9 is a novel caspase recruitment domain-containing protein that interacts with BCL10/CLAP and activates NF-kappa B. *J. Biol. Chem.* 275:41082–41086. doi:10.1074/jbc.C000726200

Borregaard, N., O.E. Sørensen, and K. Theilgaard-Mönch. 2007. Neutrophil granules: a library of innate immunity proteins. *Trends Immunol.* 28:340–345. doi:10.1016/j.it.2007.06.002

Chakravarty, S.D., G. Zhu, M.C. Tsai, V.P. Mohan, S. Marino, D.E. Kirschner, L. Huang, J. Flynn, and J. Chan. 2008. Tumor necrosis factor blockade in chronic murine tuberculosis enhances granulomatous inflammation and disorganizes granulomas in the lungs. *Infect. Immun.* 76:916–926. doi:10.1128/IAI.01011-07

De Filippo, K., R.B. Henderson, M. Laschinger, and N. Hogg. 2008. Neutrophil chemokines KC and macrophage-inflammatory protein-2 are newly synthesized by tissue macrophages using distinct TLR signaling pathways. *J. Immunol.* 180:4308–4315.

Di Liberto, D., M. Locati, N. Caccamo, A. Vecchi, S. Meraviglia, A. Salerno, G. Sireci, M. Nebuloni, N. Caceres, P.J. Cardona, et al. 2008. Role of the chemokine decoy receptor D6 in balancing inflammation, immune activation, and antimicrobial resistance in *Mycobacterium tuberculosis* infection. *J. Exp. Med.* 205:2075–2084. doi:10.1084/jem.20070608

Dorhoi, A., and S.H. Kaufmann. 2009. Fine-tuning of T cell responses during infection. *Curr. Opin. Immunol.* 21:367–377. doi:10.1016/j.coi.2009.07.004

Eruslanov, E.B., I.V. Lyadova, T.K. Kondratieva, K.B. Majorov, I.V. Scheglov, M.O. Orlova, and A.S. Apt. 2005. Neutrophil responses to *Mycobacterium tuberculosis* infection in genetically susceptible and resistant mice. *Infect. Immun.* 73:1744–1753. doi:10.1128/IAI.73.3.1744-1753.2005

Ferwerda, G., S.E. Girardin, B.J. Kullberg, L. Le Bourhis, D.J. de Jong, D.M. Langenberg, R. van Crevel, G.J. Adema, T.H. Ottenhoff, J.W. Van der Meer, and M.G. Netea. 2005. NOD2 and toll-like receptors are nonredundant recognition systems of *Mycobacterium tuberculosis*. *PLoS Pathog.* 1:279–285. doi:10.1371/journal.ppat.0010034

Fielding, C.A., R.M. McLoughlin, L. McLeod, C.S. Colmont, M. Najdovska, D. Grail, M. Ernst, S.A. Jones, N. Topley, and B.J. Jenkins. 2008. IL-6 regulates neutrophil trafficking during acute inflammation via STAT3. *J. Immunol.* 181:2189–2195.

Flesch, I., and S.H. Kaufmann. 1987. Mycobacterial growth inhibition by interferon-gamma-activated bone marrow macrophages and differential

susceptibility among strains of *Mycobacterium tuberculosis*. *J. Immunol.* 138:4408–4413.

Flynn, J.L., and J. Chan. 2001. Immunology of tuberculosis. *Annu. Rev. Immunol.* 19:93–129. doi:10.1146/annurev.immunol.19.1.93

Fortune, S.M., A. Solache, A. Jaeger, P.J. Hill, J.T. Belisle, B.R. Bloom, E.J. Rubin, and J.D. Ernst. 2004. *Mycobacterium tuberculosis* inhibits macrophage responses to IFN-gamma through myeloid differentiation factor 88-dependent and -independent mechanisms. *J. Immunol.* 172:6272–6280.

Fremond, C.M., V. Yeremeev, D.M. Nicolle, M. Jacobs, V.F. Quesniaux, and B. Ryffel. 2004. Fatal *Mycobacterium tuberculosis* infection despite adaptive immune response in the absence of MyD88. *J. Clin. Invest.* 114:1790–1799.

Fremond, C.M., D. Togbe, E. Doz, S. Rose, V. Vasseur, I. Maillet, M. Jacobs, B. Ryffel, and V.F. Quesniaux. 2007. IL-1 receptor-mediated signal is an essential component of MyD88-dependent innate response to *Mycobacterium tuberculosis* infection. *J. Immunol.* 179:1178–1189.

Gandotra, S., S. Jang, P.J. Murray, P. Salgame, and S. Ehrt. 2007. Nucleotide-binding oligomerization domain protein 2-deficient mice control infection with *Mycobacterium tuberculosis*. *Infect. Immun.* 75:5127–5134. doi:10.1128/IAI.00458-07

Garlanda, C., D. Di Liberto, A. Vecchi, M.P. La Manna, C. Buracchi, N. Caccamo, A. Salerno, F. Dieli, and A. Mantovani. 2007. Damping excessive inflammation and tissue damage in *Mycobacterium tuberculosis* infection by Toll IL-1 receptor 8/single Ig IL-1-related receptor, a negative regulator of IL-1/TLR signaling. *J. Immunol.* 179:3119–3125.

Geissmann, F., S. Jung, and D.R. Littman. 2003. Blood monocytes consist of two principal subsets with distinct migratory properties. *Immunity.* 19:71–82. doi:10.1016/S1074-7613(03)00174-2

Glocker, E.O., A. Hennigs, M. Nabavi, A.A. Schäffer, C. Woellner, U. Salzer, D. Pfeifer, H. Veelken, K. Warnatz, F. Tahami, et al. 2009. A homozygous CARD9 mutation in a family with susceptibility to fungal infections. *N. Engl. J. Med.* 361:1727–1735. doi:10.1056/NEJMoa0810719

Grattendick, K., R. Stuart, E. Roberts, J. Lincoln, S.S. Lefkowitz, A. Bollen, N. Moguilevsky, H. Friedman, and D.L. Lefkowitz. 2002. Alveolar macrophage activation by myeloperoxidase: a model for exacerbation of lung inflammation. *Am. J. Respir. Cell Mol. Biol.* 26:716–722.

Gross, O., A. Gewies, K. Finger, M. Schäfer, T. Sparwasser, C. Peschel, I. Förster, and J. Ruland. 2006. Card9 controls a non-TLR signalling pathway for innate anti-fungal immunity. *Nature.* 442:651–656. doi:10.1038/nature04926

Gross, O., H. Poeck, M. Bscheider, C. Dostert, N. Hannesschläger, S. Endres, G. Hartmann, A. Tardivel, E. Schweighoffer, V. Tybulewicz, et al. 2009. Syk kinase signalling couples to the Nlrp3 inflammasome for anti-fungal host defence. *Nature.* 459:433–436. doi:10.1038/nature07965

Hara, H., C. Ishihara, A. Takeuchi, T. Imanishi, L. Xue, S.W. Morris, M. Inui, T. Takai, A. Shibuya, S. Saijo, et al. 2007. The adaptor protein CARD9 is essential for the activation of myeloid cells through ITAM-associated and Toll-like receptors. *Nat. Immunol.* 8:619–629. doi:10.1038/ni1466

Hölscher, C., N. Reiling, U.E. Schaible, A. Hölscher, C. Bathmann, D. Korbel, I. Lenz, T. Sonntag, S. Kröger, S. Akira, et al. 2008. Containment of aerogenic *Mycobacterium tuberculosis* infection in mice does not require MyD88 adaptor function for TLR2, -4 and -9. *Eur. J. Immunol.* 38:680–694. doi:10.1002/eji.200736458

Hsu, Y.M., Y. Zhang, Y. You, D. Wang, H. Li, O. Duramad, X.F. Qin, C. Dong, and X. Lin. 2007. The adaptor protein CARD9 is required for innate immune responses to intracellular pathogens. *Nat. Immunol.* 8:198–205. doi:10.1038/ni1426

Ishii, K.J., S. Koyama, A. Nakagawa, C. Coban, and S. Akira. 2008. Host innate immune receptors and beyond: making sense of microbial infections. *Cell Host Microbe.* 3:352–363. doi:10.1016/j.chom.2008.05.003

Ishikawa, E., T. Ishikawa, Y.S. Morita, K. Toyonaga, H. Yamada, O. Takeuchi, T. Kinoshita, S. Akira, Y. Yoshikai, and S. Yamasaki. 2009. Direct recognition of the mycobacterial glycolipid, trehalose dimycolate, by C-type lectin Mincle. *J. Exp. Med.* 206:2879–2888. doi:10.1084/jem.20091750

Keller, C., R. Hoffmann, R. Lang, S. Brandau, C. Hermann, and S. Ehlers. 2006. Genetically determined susceptibility to tuberculosis in mice causally involves accelerated and enhanced recruitment of granulocytes. *Infect. Immun.* 74:4295–4309. doi:10.1128/IAI.00057-06

Khader, S.A., S. Partida-Sanchez, G. Bell, D.M. Jelley-Gibbs, S. Swain, J.E. Pearl, N. Ghilardi, F.J. Desauvage, F.E. Lund, and A.M. Cooper. 2006. Interleukin 12p40 is required for dendritic cell migration and T cell priming after *Mycobacterium tuberculosis* infection. *J. Exp. Med.* 203:1805–1815. doi:10.1084/jem.20052545

Kipnis, A., R.J. Basaraba, I.M. Orme, and A.M. Cooper. 2003. Role of chemokine ligand 2 in the protective response to early murine pulmonary tuberculosis. *Immunology.* 109:547–551. doi:10.1046/j.1365-2567.2003.01680.x

Kono, H., and K.L. Rock. 2008. How dying cells alert the immune system to danger. *Nat. Rev. Immunol.* 8:279–289. doi:10.1038/nri2215

Koziol-Montewka, M., A. Kolodziejek, and J. Oles. 2004. Study on myeloperoxidase role in antituberculous defense in the context of cytokine activation. *Inflammation.* 28:53–58. doi:10.1023/B:IFLA.0000033020.28446.a6

Kursar, M., M. Koch, H.W. Mittrücker, G. Nouailles, K. Bonhagen, T. Kamradt, and S.H. Kaufmann. 2007. Cutting Edge: Regulatory T cells prevent efficient clearance of *Mycobacterium tuberculosis*. *J. Immunol.* 178:2661–2665.

LeibundGut-Landmann, S., O. Gross, M.J. Robinson, F. Osorio, E.C. Slack, S.V. Tsoni, E. Schweighoffer, V. Tybulewicz, G.D. Brown, J. Ruland, and C. Reis e Sousa. 2007. Syk- and CARD9-dependent coupling of innate immunity to the induction of T helper cells that produce interleukin 17. *Nat. Immunol.* 8:630–638. doi:10.1038/ni1460

Medzhitov, R. 2007. Recognition of microorganisms and activation of the immune response. *Nature.* 449:819–826. doi:10.1038/nature06246

Morimoto, K., W.J. Janssen, M.B. Fessler, K.A. McPhillips, V.M. Borges, R.P. Bowler, Y.Q. Xiao, J.A. Kench, P.M. Henson, and R.W. Vandivier. 2006. Lovastatin enhances clearance of apoptotic cells (efferocytosis) with implications for chronic obstructive pulmonary disease. *J. Immunol.* 176:7657–7665.

Nathan, C.F. 1987. Neutrophil activation on biological surfaces. Massive secretion of hydrogen peroxide in response to products of macrophages and lymphocytes. *J. Clin. Invest.* 80:1550–1560. doi:10.1172/JCI113241

Pan, H., B.S. Yan, M. Rojas, Y.V. Shebzukhov, H. Zhou, L. Kobzik, D.E. Higgins, M.J. Daly, B.R. Bloom, and I. Kramnik. 2005. Ipr1 gene mediates innate immunity to tuberculosis. *Nature.* 434:767–772. doi:10.1038/nature03419

Poeck, H., M. Bscheider, O. Gross, K. Finger, S. Roth, M. Rebsamen, N. Hannesschläger, M. Schlee, S. Rothenfusser, W. Barchet, et al. 2010. Recognition of RNA virus by RIG-I results in activation of CARD9 and inflammasome signaling for interleukin 1 beta production. *Nat. Immunol.* 11:63–69. doi:10.1038/ni.1824

Quesniaux, V., C. Fremond, M. Jacobs, S. Parida, D. Nicolle, V. Yeremeev, F. Bihl, F. Erard, T. Botha, M. Drennan, et al. 2004. Toll-like receptor pathways in the immune responses to mycobacteria. *Microbes Infect.* 6:946–959. doi:10.1016/j.micinf.2004.04.016

Reiling, N., C. Hölscher, A. Fehrenbach, S. Kröger, C.J. Kirschning, S. Goyert, and S. Ehlers. 2002. Cutting edge: Toll-like receptor (TLR)2- and TLR4-mediated pathogen recognition in resistance to airborne infection with *Mycobacterium tuberculosis*. *J. Immunol.* 169:3480–3484.

Reiling, N., S. Ehlers, and C. Hölscher. 2008. MyDths and un-TOLLed truths: sensor, instructive and effector immunity to tuberculosis. *Immunol. Lett.* 116:15–23. doi:10.1016/j.imlet.2007.11.015

Rothfuchs, A.G., A. Bafica, C.G. Feng, J.G. Egen, D.L. Williams, G.D. Brown, and A. Sher. 2007. Dectin-1 interaction with *Mycobacterium tuberculosis* leads to enhanced IL-12p40 production by splenic dendritic cells. *J. Immunol.* 179:3463–3471.

Schnappinger, D., G.K. Schoolnik, and S. Ehrt. 2006. Expression profiling of host pathogen interactions: how *Mycobacterium tuberculosis* and the macrophage adapt to one another. *Microbes Infect.* 8:1132–1140. doi:10.1016/j.micinf.2005.10.027

Scott, H.M., and J.L. Flynn. 2002. *Mycobacterium tuberculosis* in chemokine receptor 2-deficient mice: influence of dose on disease progression. *Infect. Immun.* 70:5946–5954. doi:10.1128/IAI.70.11.5946-5954.2002

Seiler, P., P. Aichele, B. Raupach, B. Odermatt, U. Steinhoff, and S.H. Kaufmann. 2000. Rapid neutrophil response controls fast-replicating

intracellular bacteria but not slow-replicating *Mycobacterium tuberculosis*. *J. Infect. Dis.* 181:671–680. doi:10.1086/315278

Seimon, T.A., A. Obstfeld, K.J. Moore, D.T. Golenbock, and I. Tabas. 2006. Combinatorial pattern recognition receptor signaling alters the balance of life and death in macrophages. *Proc. Natl. Acad. Sci. USA*. 103:19794–19799. doi:10.1073/pnas.0609671104

Shi, S., C. Nathan, D. Schnappinger, J. Drenkow, M. Fuortes, E. Block, A. Ding, T.R. Gingeras, G. Schoolnik, S. Akira, et al. 2003. MyD88 primes macrophages for full-scale activation by interferon-gamma yet mediates few responses to *Mycobacterium tuberculosis*. *J. Exp. Med.* 198:987–997. doi:10.1084/jem.20030603

Tailleux, L., S.J. Waddell, M. Pelizzola, A. Mortellaro, M. Withers, A. Tanne, P.R. Castagnoli, B. Gicquel, N.G. Stoker, P.D. Butcher, et al. 2008. Probing host pathogen cross-talk by transcriptional profiling of both *Mycobacterium tuberculosis* and infected human dendritic cells and macrophages. *PLoS One*. 3:e1403. doi:10.1371/journal.pone.0001403

Trinchieri, G., and A. Sher. 2007. Cooperation of Toll-like receptor signals in innate immune defence. *Nat. Rev. Immunol.* 7:179–190. doi:10.1038/nri2038

Ueda, Y., D.W. Cain, M. Kuraoka, M. Kondo, and G. Kelsoe. 2009. IL-1R type I-dependent hemopoietic stem cell proliferation is necessary for inflammatory granulopoiesis and reactive neutrophilia. *J. Immunol.* 182:6477–6484. doi:10.4049/jimmunol.0803961

Vandivier, R.W., V.A. Fadok, P.R. Hoffmann, D.L. Bratton, C. Penvari, K.K. Brown, J.D. Brain, F.J. Accurso, and P.M. Henson. 2002. Elastase-mediated phosphatidylserine receptor cleavage impairs apoptotic cell clearance in cystic fibrosis and bronchiectasis. *J. Clin. Invest.* 109:661–670.

Wengner, A.M., S.C. Pitchford, R.C. Furze, and S.M. Rankin. 2008. The coordinated action of G-CSF and ELR + CXC chemokines in neutrophil mobilization during acute inflammation. *Blood*. 111:42–49. doi:10.1182/blood-2007-07-099648

Werninghaus, K., A. Babiak, O. Gross, C. Hölscher, H. Dietrich, E.M. Agger, J. Mages, A. Mocsai, H. Schoenen, K. Finger, et al. 2009. Adjuvanticity of a synthetic cord factor analogue for subunit *Mycobacterium tuberculosis* vaccination requires FcRgamma-Syk-Card9-dependent innate immune activation. *J. Exp. Med.* 206:89–97. doi:10.1084/jem.20081445

WHO. 2008. Tuberculosis Facts www.who.int/tb/publications/global_report/en. WHO.

Yadav, M., and J.S. Schorey. 2006. The beta-glucan receptor dectin-1 functions together with TLR2 to mediate macrophage activation by mycobacteria. *Blood*. 108:3168–3175. doi:10.1182/blood-2006-05-024406

Yang, Y., C. Yin, A. Pandey, D. Abbott, C. Sassetti, and M.A. Kelliher. 2007. NOD2 pathway activation by MDP or *Mycobacterium tuberculosis* infection involves the stable polyubiquitination of Rip2. *J. Biol. Chem.* 282:36223–36229. doi:10.1074/jbc.M703079200

Zhang, X., L. Majlessi, E. Deriaud, C. Leclerc, and R. Lo-Man. 2009. Coactivation of Syk kinase and MyD88 adaptor protein pathways by bacteria promotes regulatory properties of neutrophils. *Immunity*. 31:761–771. doi:10.1016/j.immuni.2009.09.016